

Beam Flattener Design for High-Energy Radiographic Inspection

Robert Grandin

Dr. Thomas Rudolphi, Faculty Advisor

Department of Aerospace Engineering

Senior Symposium

Iowa State University

December 2009



- Radiographic Inspection
- Design Problem
- Solution Approach
 - Beam Modeling
 - Hardware Modeling
 - Flattener Definition
- Ideal Solution
- Feasible Design
- Performance Analysis
- Conclusions

- **Radiographic Inspection**
- Design Problem
- Solution Approach
 - Beam Modeling
 - Hardware Modeling
 - Flattener Definition
- Ideal Solution
- Feasible Design
- Performance Analysis
- Conclusions

- Radiographic inspection is a non-destructive inspection method using X-radiation to penetrate an object
 - Used to inspect for subsurface anomalies inside an object
 - Energy and quantity of X-ray photons determined by density and thickness of object being inspected

| Inspection | Photon Energy | Dose |
|----------------|---------------|------------|
| Medical, Chest | 150 keV | 0.050 Rem |
| Rocket Motor | 15,000 keV | 50,000 Rem |



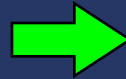
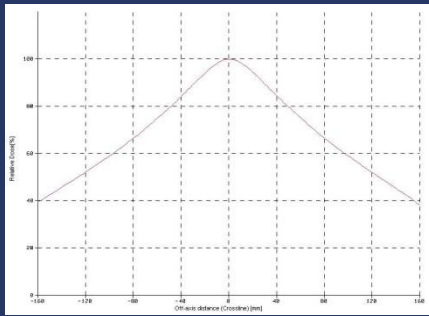
- Inspections are based on interpreting exposure differences on film
 - White: high-density material
 - Dark: low-density material
- Radiation is absorbed exponentially through material
- When designing an inspection, half-value layers (HVL) are used to compare thicknesses
 - 1 HVL is the thickness of material required to reduce the original radiation intensity by half
 - 2 HVLs reduce the intensity to 25% of the original value
 - Allows for meaningful comparisons to be made between materials of different densities



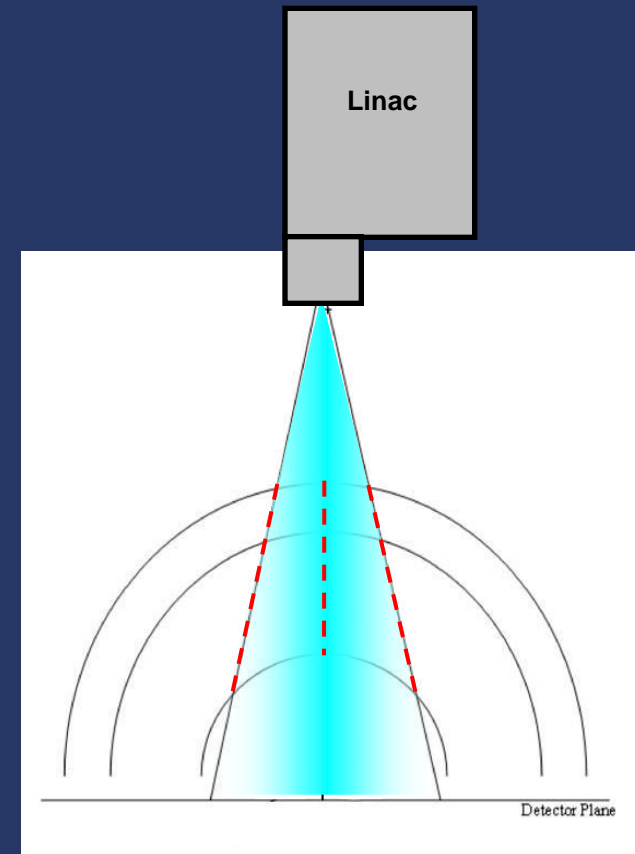
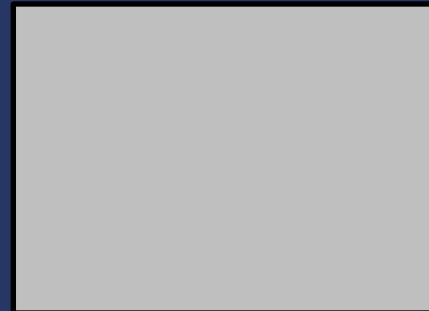
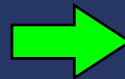
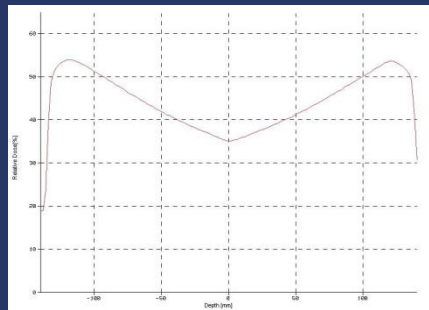
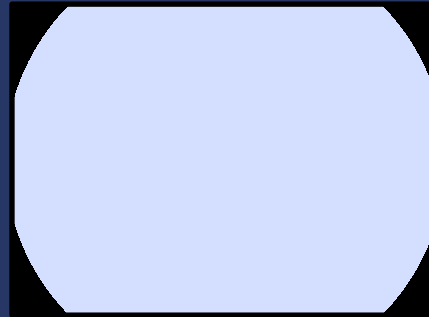
- High photon energies required to penetrate thick rocket motor components
 - Increased energy produces greater penetrating power
 - Also reduces contrast as compared to low-energy exposures
- Other high-energy complications
 - Scatter: Secondary radiation generated by the component when bombarded by high-energy radiation
 - Clouds film
 - Free-neutron generation
 - Damages electronic components
- Production of high-energy radiation requires the use of a linear accelerator
- Beam flatteners are used to modify radiation intensity profile to improve inspection quality
 - Adjust intensity to match component geometry

- What is a beam flattener?
 - Accounts for part geometry to create even radiation intensity distribution at detector
 - Normalizes image over large area to ensure inspection meets process requirements and to facilitate evaluation of radiographs

Beam intensity profile

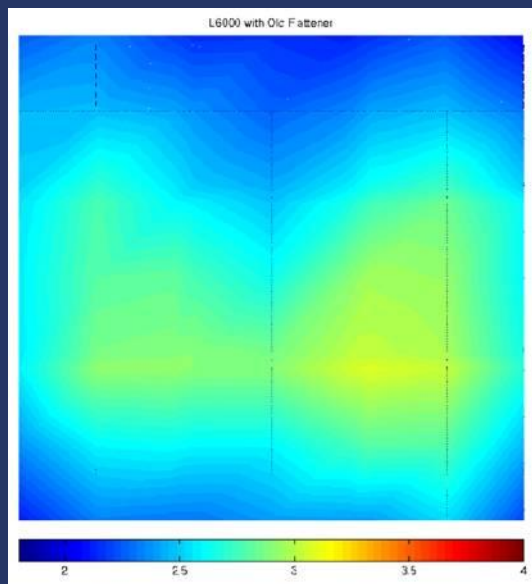


Resultant film exposure

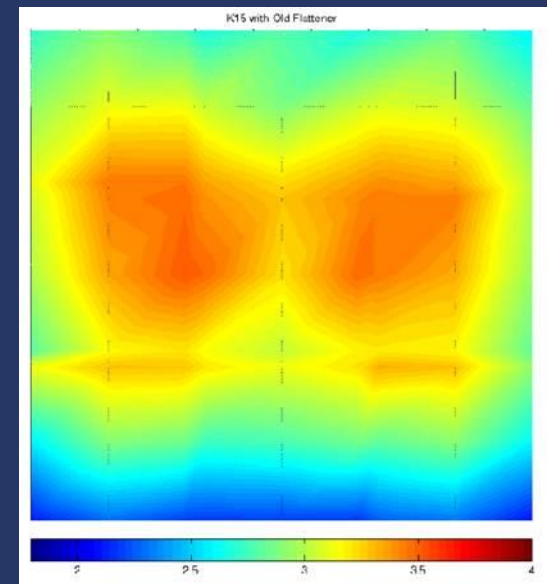


- Radiographic Inspection
- **Design Problem**
- Solution Approach
 - Beam Modeling
 - Hardware Modeling
 - Flattener Definition
- Ideal Solution
- Feasible Design
- Performance Analysis
- Conclusions

- In 2007 ATK Space Systems began the process of replacing two linear accelerators used to inspect Space Shuttle solid rocket boosters
- The new accelerators have different radiation intensity profiles from the old accelerators, but are used to inspect the same hardware
 - Caused an increase in range of exposure values on film, which mandated additional exposures (time and money) and impacted production schedule



Film exposure range for L6000 (old accelerator)

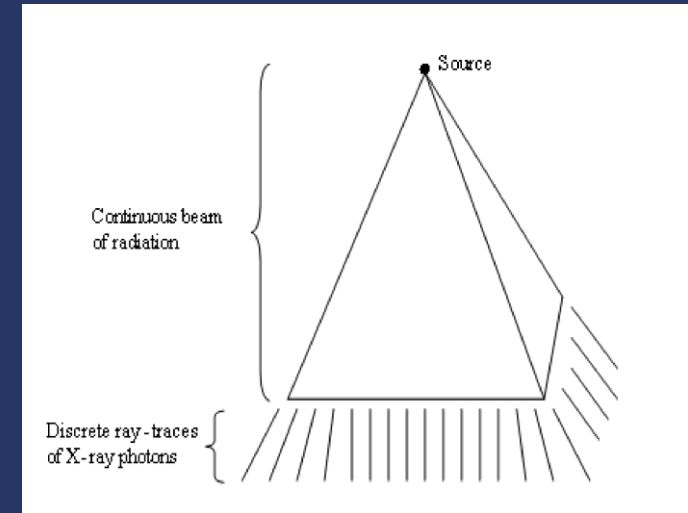


Film exposure range for K15 (new accelerator)

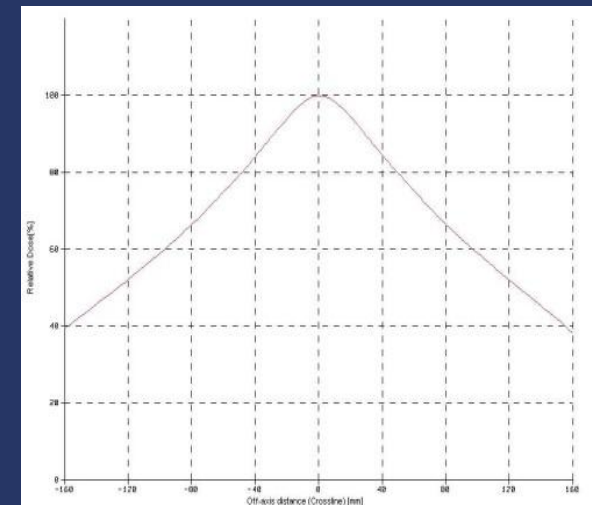
- Radiographic Inspection
- Design Problem
- **Solution Approach**
 - Beam Modeling
 - Hardware Modeling
 - Flattener Definition
- Ideal Solution
- Feasible Design
- Performance Analysis
- Conclusions

- Beam modeled as a discrete number of ray-traces
- Applied numerical analysis to each discrete ray instead of developing a closed-form solution
 - Sufficiently-large number of rays provides quality beam representation
 - Closed-form solution unnecessarily complex
- Assumptions
 - Rays travel in straight lines (no refraction at material interfaces)
 - Rays emitted from a point source
- Intensity varied according to measured beam intensity profile

Beam model

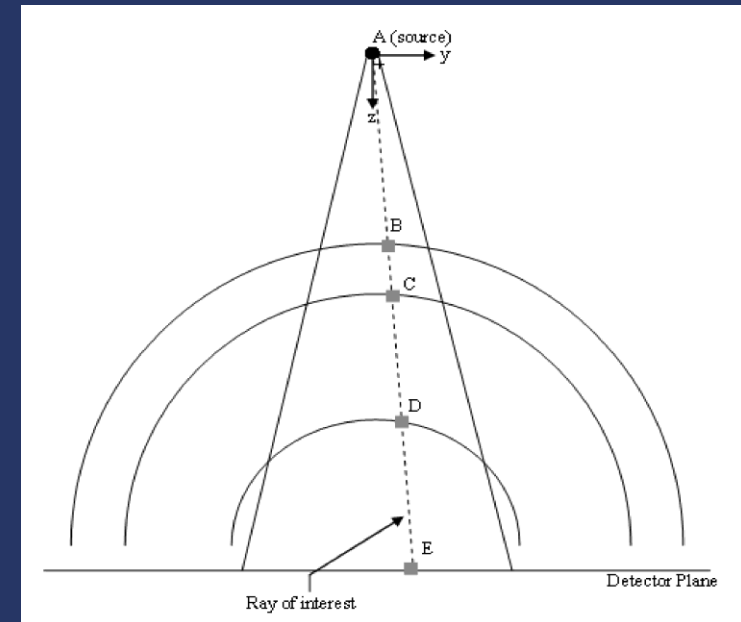


Measured beam intensity profile



- Solution also required development of mathematical model of hardware geometry and its interaction with the discrete rays
- Calculated the distance each ray travels through each material
 - Determine number of HVLs included in this distance
- **Ultimate solution**: Total HVLs encountered by each ray must be equal in order to produce an even exposure on the film
 - Combine for beam model with those for hardware model to solve for total HVLs
 - All rays must have material added in order to equalize HVLs
 - Profile of added material defined contour of beam flattener

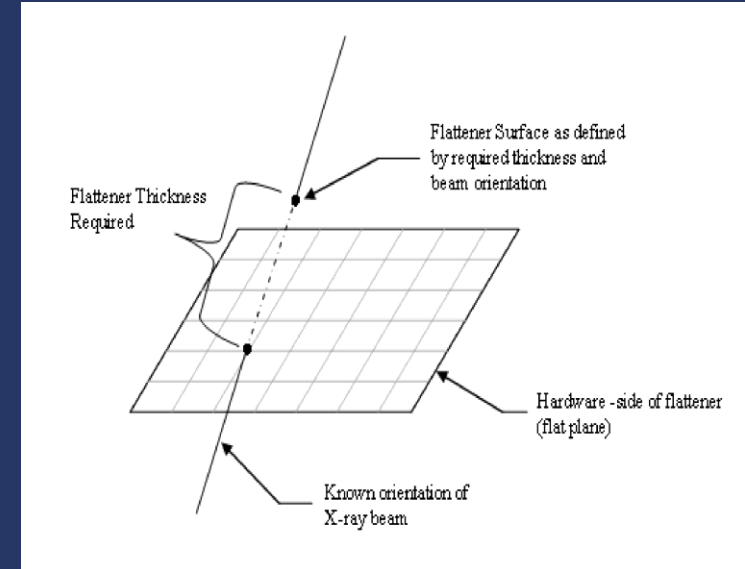
Hardware model



Solution Approach – Flattener Definition

- Front face of flattener defined to be planar due to mounting requirements within the linac
- Both ray orientation and required material addition are known
- Combine known orientation and thickness to determine back surface of flattener

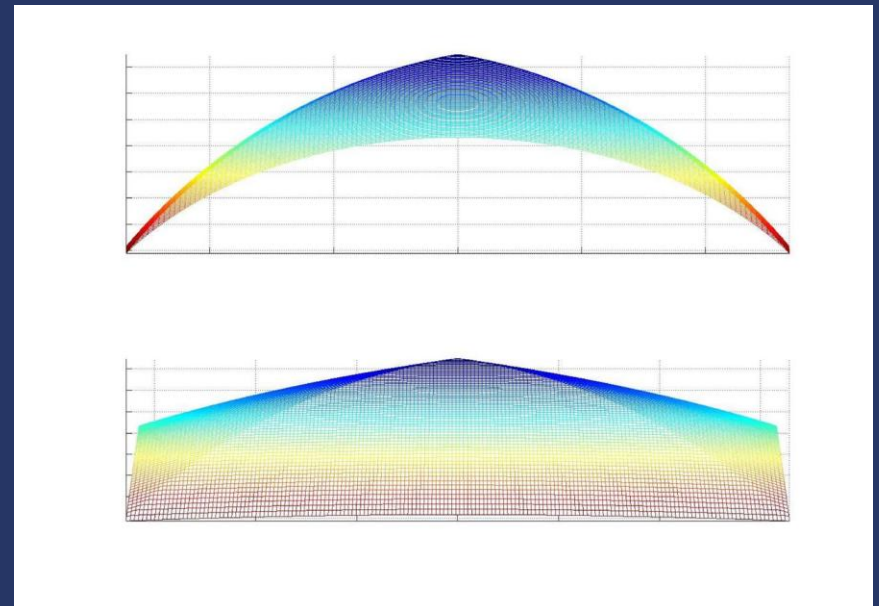
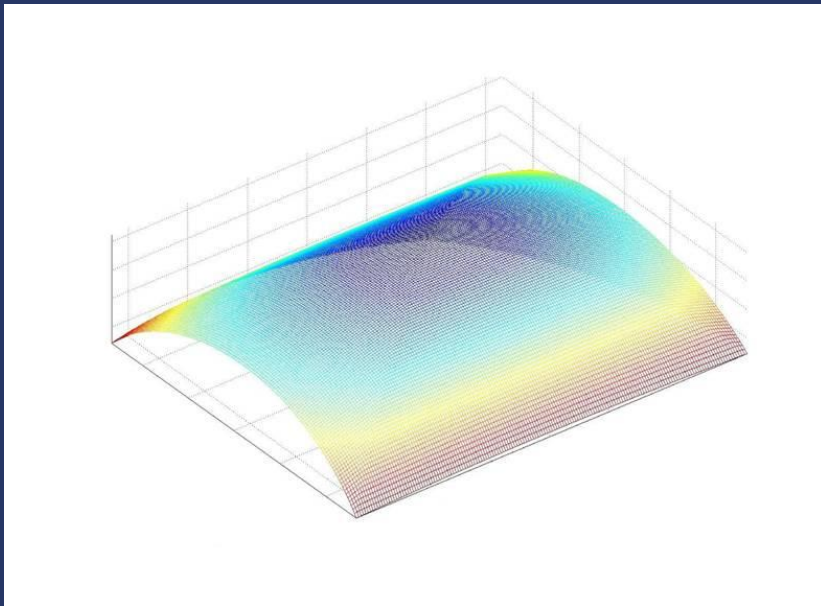
Beam flattener model



- Radiographic Inspection
- Design Problem
- Solution Approach
 - Beam Modeling
 - Hardware Modeling
 - Flattener Definition
- **Ideal Solution**
- Feasible Design
- Performance Analysis
- Conclusions

- High resolution beam model produced flattener profile with over 20,000 data points
- Curves appear consistent with components inspected (“gut feel” test)
- Ridges due to beam profile model

Numerically-generated, ideal solution for profile of beam flattener



- Developed new problem: ideal solution was too complicated to fabricate
 - Due to space constraints, tungsten was chosen as flattener material
 - Machining tungsten to compound curves requires several days' effort on 5-axis computer numerical control (CNC) machines
 - Neither budget nor schedule permitted the resources required
- Solution to this new problem: reduce the complexity
 - Take thousands of faces and reduce them to 12
 - Allows for quicker production on more readily-available machines
 - Satisfies both time and money constraints

- Radiographic Inspection
- Design Problem
- Solution Approach
 - Beam Modeling
 - Hardware Modeling
 - Flattener Definition
- Ideal Solution
- **Feasible Design**
- Performance Analysis
- Conclusions

- Identified the most critical dimensions of ideal solution and interpolated between those points
- More facets than old flattener, allowing for improved compensating ability when used to inspect rocket motor hardware

New, simplified beam flattener

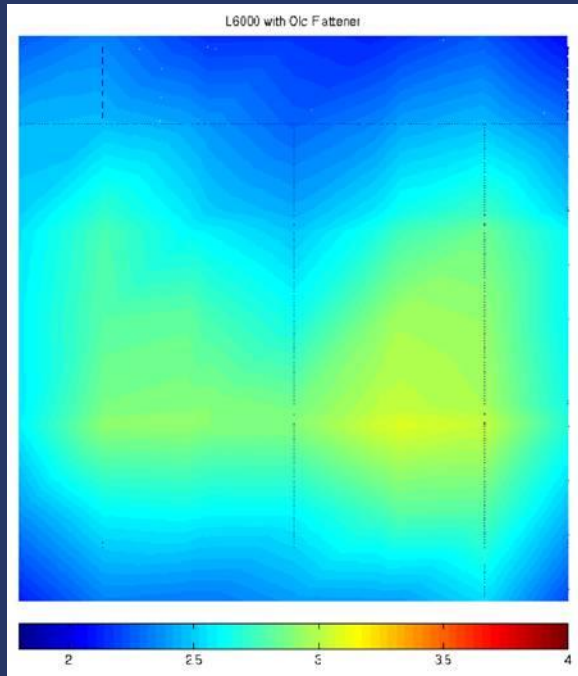


- Radiographic Inspection
- Design Problem
- Solution Approach
 - Beam Modeling
 - Hardware Modeling
 - Flattener Definition
- Ideal Solution
- Feasible Design
- **Performance Analysis**
- Conclusions

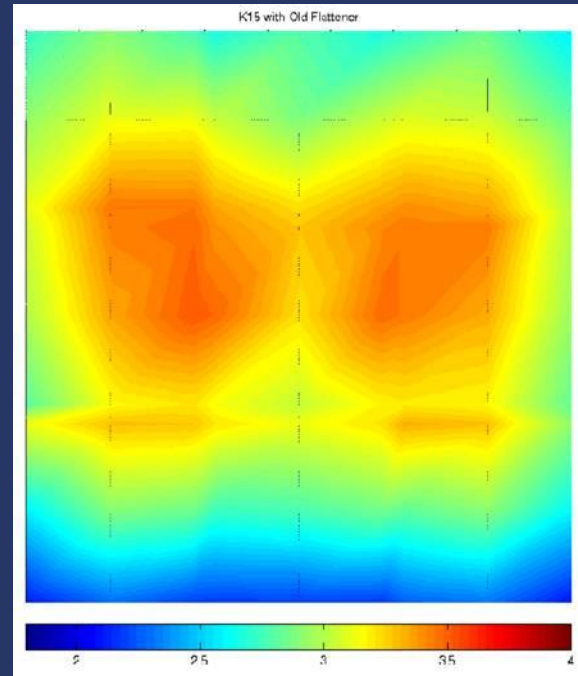
- Success of the final solution (simplified beam flattener) had to be determined by the resultant film exposure range
 - Successful solution would have smaller film exposure range and smaller standard deviation of film exposure values
 - Compared three combinations of accelerators and flatteners
- Measured film exposure at multiple locations across the resultant radiographic film array

| Accelerator | L6000 | K15 | K15 |
|---------------------------|---------------------|---------------|------------------|
| Beam flattener | Original | Original | New (simplified) |
| Range | 1.02 | 1.42 | 0.91 |
| Standard Deviation | 0.26 | 0.37 | 0.20 |
| Reference | Historical baseline | First attempt | Final solution |

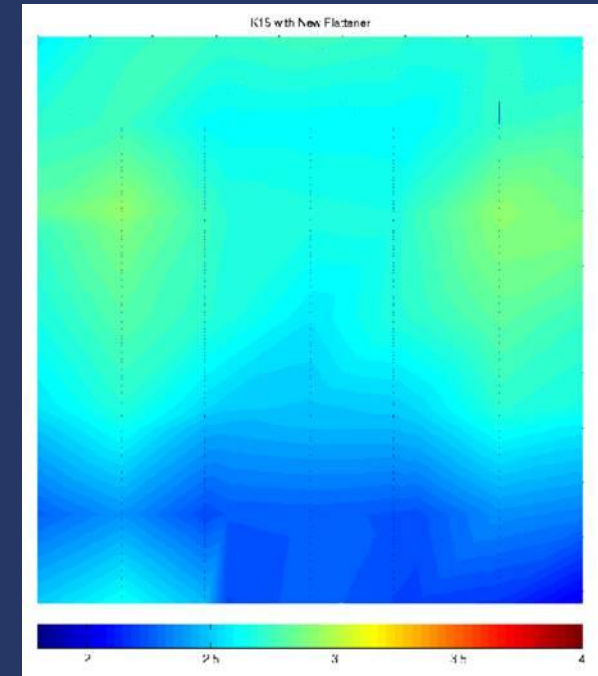
- Film exposure plots of the three combinations of accelerators and flatteners



L6000, original flattener,
historical baseline



K15, original flattener, first
attempt



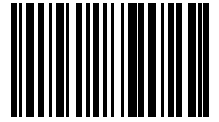
K15, new flattener,
final solution

- Radiographic Inspection
- Design Problem
- Solution Approach
 - Beam Modeling
 - Hardware Modeling
 - Flattener Definition
- Ideal Solution
- Feasible Design
- Performance Analysis
- **Conclusions**

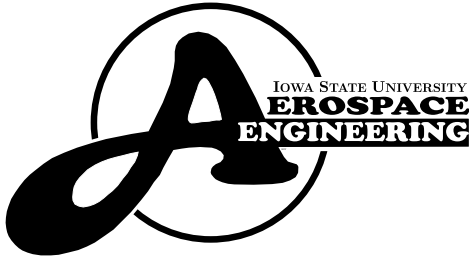
- Achieved measurable improvement over both the first attempt (K15 with old flattener) and the historical standard (L6000 with old flattener)
- The smaller film density range and standard deviation produced by the new flattener resulted in a more consistent, predictable inspection process
 - Eliminated the need to take two separate exposures for every view
 - Saves time and money and improves ability to deliver components for next step in manufacturing process
- Results deemed successful enough to warrant the application of this design process to other component inspections

- ATK Space Systems
 - Volker Teller - Manager, RSRM Nondestructive Test
 - Walter Becker - Manager, RSRM Radiography
 - Michael Hassebrock – RSRM Radiography Engineering
- Iowa State University
 - Dr. Thomas Rudolphi – Faculty Advisor
 - Dr. Dale Chimenti – AerE 492 Course Instructor

Questions?



December 2009



Beam-Flattener Design for High Energy Radiographic Inspection

Robert Grandin

A technical report submitted to the Aerospace Engineering faculty
in partial fulfillment of the requirements for the course
AerE 492 — Senior Seminar

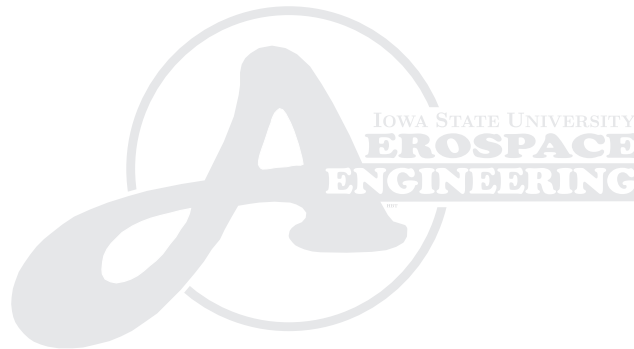
Project Advisor: Dr. Thomas Rudolphi

Iowa State University of Science and Technology
Department of Aerospace Engineering

This is to certify that this is an original work of

Robert Grandin

There is no misappropriation of another author's contributions,
including an author's ideas, information, or words.



Author

This technical report has met the
English and technical content proficiency requirements
for a formal report and is hereby approved by:

Project Advisor

TABLE OF CONTENTS

| | |
|---|----|
| LIST OF FIGURES | iv |
| ACKNOWLEDGEMENT | v |
| ABSTRACT | vi |
| CHAPTER 1 INTRODUCTION | 1 |
| 1.1 Radiography Background | 1 |
| 1.1.1 General Radiography | 1 |
| 1.1.2 High-Energy Complications | 2 |
| 1.2 Design Problem | 4 |
| 1.2.1 New Inspection Hardware, Same Inspected Components | 4 |
| 1.2.2 Constraints | 4 |
| CHAPTER 2 SOLUTION DEVELOPMENT | 5 |
| 2.1 Approach Overview | 5 |
| 2.2 Assumptions | 5 |
| 2.3 Beam Modeling | 6 |
| 2.3.1 Continuum to Discrete | 6 |
| 2.3.2 Intensity Variation | 7 |
| 2.4 Hardware Modeling | 7 |
| 2.4.1 Coordinate System | 7 |
| 2.4.2 Defining The Geometric Model | 8 |
| 2.5 Flattener Determination | 9 |
| 2.5.1 Surface Calculations | 9 |
| 2.5.2 Material Selection | 10 |
| 2.5.3 Fabrication Data | 10 |
| CHAPTER 3 FINAL DESIGN | 11 |
| 3.1 Idealized Design | 11 |
| 3.2 Design Simplification | 12 |
| 3.3 Design Performance | 13 |
| 3.3.1 Statistical Analysis | 13 |
| 3.3.2 Graphical Analysis | 13 |
| CHAPTER 4 CONCLUSIONS | 17 |
| 4.1 Quantitative | 17 |
| 4.2 Qualitative | 17 |
| 4.3 Final Verdict | 17 |
| 4.4 Future Work | 17 |
| 4.5 Significance | 18 |
| 4.5.1 Inspection Quality | 18 |
| 4.5.2 Safety | 18 |
| APPENDIX A INTERPERETING FILM EXPOSURE PLOTS | 19 |
| APPENDIX B INTERNATIONAL TRAFFIC IN ARMS INFORMATION | 20 |

LIST OF FIGURES

| | | |
|-----|---|----|
| 1.1 | X-Ray image of a human hand | 1 |
| 1.2 | Effect of a beam flattener | 3 |
| 2.1 | Discretizing the continuous cone of radiation | 6 |
| 2.2 | Beam intensity profile | 7 |
| 2.3 | Points of interest in modeling the hardware | 8 |
| 2.4 | Determining the flattener top surface | 10 |
| 3.1 | Isometric view of fine-mesh model | 11 |
| 3.2 | Orthogonal views of the simplified flattener design | 12 |
| 3.3 | Photo of new beam flattener | 12 |
| 3.4 | Exposure data collection locations | 13 |
| 3.5 | L6000 with old beam flattener surface plot | 14 |
| 3.6 | K15 with old beam flattener surface plot | 15 |
| 3.7 | K15 with new beam flattener surface plot | 16 |
| 3.8 | Exposure Comparison Plots | 16 |

ACKNOWLEDGEMENT

The following individuals have been instrumental in both the execution and documentation of this project. Without their assistance neither the work described herein nor this documentation would have been possible.

ATK Space Systems

- Volker Teller – RSRM NDT Manager
- Walter Becker – RSRM NDT Radiography Manager
- Michael Hassebrock – RSRM Radiography Engineering
- Dale Francis – RSRM Radiography Engineering
- Jennie Campbell – Export/Import Control Officer
- Quinn Howard – Export/Import Control Officer

Iowa State University

- Dr. Thomas Rudolphi – Project Advisor
- Dr. Dale Chimenti – AerE 492 Course Instructor

ABSTRACT

This report documents the work done to develop a beam flattener for use in the inspection of rocket motors at ATK Space Systems' Utah facilities. The following pages provide a brief introduction to the necessity of this project, comprehensive description of the design methodology, and experientially-based conclusions regarding project success.

CHAPTER 1 INTRODUCTION

1.1 Radiography Background

Before presenting the design problem that comprises the purpose of this project, some principles of radiography must first be covered. Both general radiography topics and high-energy considerations will be introduced so as to avoid further confusion in this report. Before considering topics specific to higher energies, radiography itself will be introduced and briefly explained.

1.1.1 General Radiography

Radiographic inspection is based upon differences in film exposure which are then interpreted by trained technicians. As a result, an even background exposure is desirable so as to make exposure differences more-easily distinguishable. Radiographs range from near-white, in locations of low exposure, to near-black, in locations of high exposure. Lighter shades indicate that the radiation either passed through a greater thickness of material, or a material of greater density, and for this reason dense bones show up as white on the image of the hand shown in fig. 1.1 while the surrounding soft tissue appears darker.



Figure 1.1 X-Ray image of a human hand

X-ray intensity decreases exponentially as it passes through more and more material. This absorption due to thick and/or dense materials is countered by either increasing exposure time or increasing the energy level of the x-rays. Increasing the energy level provides the radiation with greater penetrating power through a material. Lower energy levels produce higher-contrast images, so the image quality sacrifice due to increasing the energy level must be balanced against a potential cost savings resulting from shorter exposure times.

One issue that adds complications to the modeling of the radiation beam is due to its varying intensity as a function of spatial location. Radiation exits the source, whether it be an isotope, linear accelerator, or some other source, with a particular pattern of intensity. In the case of the linear accelerator of interest here, the intensity is greatest in the center and decreases towards the edges of the radiation beam and resembles the shape of a pyramid. With the more-intense

radiation at the center of the beam a profile like this is well-suited to inspect objects that are thicker in their middle than at their edges.

Often times, however, the geometry of the components being inspected is not ideal for the intensity pattern of the radiation source. A simple example of this is a flat plate. From the perspective of the radiation photons, the distance traveled through the plate at the edges of the beam is greater than the distance through the middle and is due to the varying angle at which the photon hits the surface. In the case of complex geometries, these varying distances can be so diverse that the beam's intensity profile must be altered so as to improve its compatibility with the component. Adjusting the intensity profile is accomplished using what is called a "beam flattener." If the inspection is focused on a small number of components this flattener can also take into account the part geometry to further optimize film exposures. The methodology outlined here will pursue this path of combining both beam intensity profile with part geometry to create an optimal beam flattener. Technicians' ability to accurately interpret radiographs depends upon their ability to discern exposure differences on the radiographs. The use of a beam flattener provides a more even background exposure that allows anomalies to be better-detected due to their contrast against the background. A graphical representation of the purpose of a beam flattener can be found in fig. 1.2. In this figure one can observe how the peak of the intensity profile in the no flattener case causes over-exposure in the center of the film and under-exposure on the edges. Additionally, it is observed how the including of a beam flattener affects both the beam intensity profile and the resulting exposure.

One final concept to introduce is that of half-value layers (HVLs). One HVL is the thickness of material that reduces the radiation intensity to one-half of its original intensity. Two HVLs would reduce the beam to 25 percent of its original strength, three would result in 12.5 percent, and so on. This concept of HVLs allows for useful comparisons between materials. Due to various materials having different absorption characteristics, direct comparison of thicknesses does not provide a useful comparison in regards to radiation absorption. If, however, the comparison is now made in terms of HVLs it becomes possible to meaningfully compare different materials and thicknesses. HVLs effectively non-dimensionalize the problem and allow for the legitimate comparison of dramatically-different materials.

1.1.2 High-Energy Complications

While the concepts introduced above remain valid for all radiography, the energies required for rocket motor inspection introduce additional complications. Radiographic inspection of rocket motors requires high energy levels in order to penetrate their thick, dense components. At these energies the collisions between the radiation photons and the material being inspected cause more radiation to be produced. This phenomenon is known as "scatter radiation" and causes the resulting image to be cloudy and less-defined.

Additionally, at high energy levels the collision of radiation photons with various materials will force neutrons to be emitted. Compared to the usual photons, neutrons possess much more mass and pose serious threats to both image quality and electronic equipment. Many metals have particularly high neutron emission rates while many plastics provide good neutron absorption abilities.

The addition of a tungsten beam flattener to the inspection setup posed potential problems in regards to both scatter radiation and neutron absorption. Scatter effects and neutron emission could be minimized by keeping the flattener as thin as possible, but the potential for problems remained. Computer modeling of the radiation allows for a general estimate of these effects, but due to the modeling difficulties associated with these phenomena, only through validation testing would the actual effects on the inspection be realized and quantified.

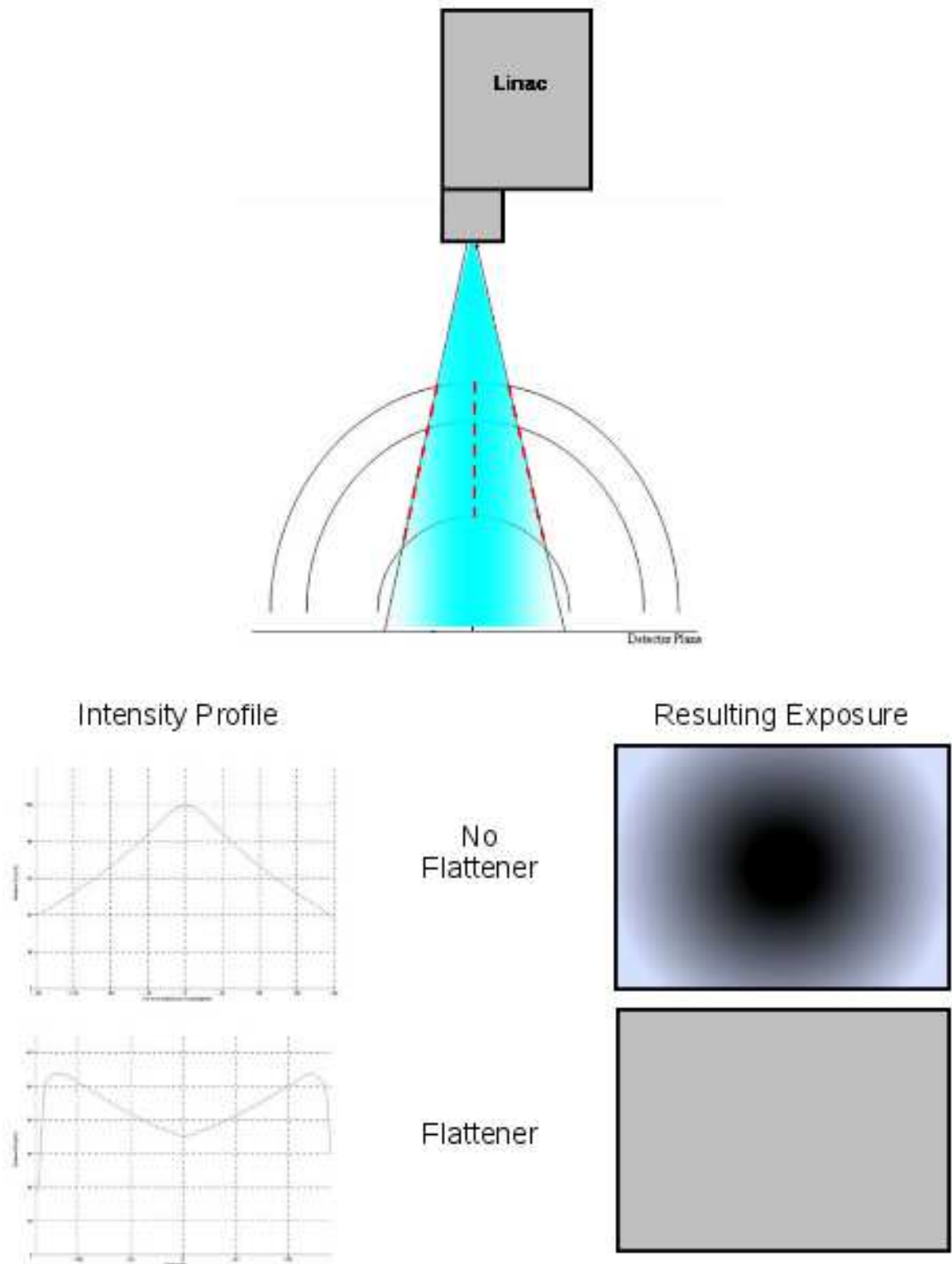


Figure 1.2 Effect of a beam flattener

1.2 Design Problem

1.2.1 New Inspection Hardware, Same Inspected Components

In 2007 ATK Space Systems began the process of replacing two linear accelerators used in the inspection of the Space Shuttle Reusable Solid Rocket Motor (RSRM). The new accelerators, known by their “K15” model numbers, are comparable in radiation output and energy but are not identical to their predecessors, known by their “L6000” model numbers. These differences between the old and new had to be understood, quantified, and corrected for, if necessary.

Due to the radiation profiles of the new machines, the existing beam flattener was found to not adequately adapt this radiation to the existing RSRM hardware. Qualification testing performed on the newly-installed accelerator revealed that while the image standards were still met, inspection quality and robustness did not measure up to the considered “normal” values. While this change did not violate inspection standards, it was in the best interests of all parties involved to take corrective action that would bring the image quality on-par, if not better than, what had been delivered for the past two decades. Another consideration that needed to be addressed was the effect of the increased exposure range on the production budget and schedule. The exposure ranges observed with the existing beam flattener in the new accelerator required additional exposures to be taken for each inspection view, which increased both the time required for inspection and the associated cost.

The design and installation of a new beam flattener was chosen to address these issues. Due to the high-energy considerations listed in sec. 1.1.2, the design of a beam flattener is often an iterative process. As a result, no beam flatteners are available “off-the-shelf” and ATK was placed in the position of needing to design a replacement flattener.

1.2.2 Constraints

In addition to having no commercially available solution, other constraints were imposed upon the project. As introduced in sec. 1.1.2, material thickness would ideally be kept to a minimum so as to reduce the negative effects of the flattener’s presence. Additionally, less material would also translate into a cost savings in both material and fabrication labor.

Another constraint, discussed more-fully in sec. 3.2, dealt with the actual fabrication of the flattener. The computational power of today’s computers allows for the generation of designs that are simply infeasible to produce. Such was the case with this flattener. The original design had over 20,000 points defining its top surface and this number had to be brought down to the order of between ten and twenty for the flattener to meet manufacturing budgets and schedules.

And finally, time was of great importance during this design. There was no way to know how the existing beam flattener would perform in the new machine until the first test shots were taken. This meant that the design and fabrication of the new beam flattener had to happen quickly so as to not adversely affect the installation schedule of the K15.

The following chapters will detail the approach taken to design a new beam flattener for installation in the new accelerator, an evaluation of the design solution as compared to manufacturability, the feasible solution, and an analysis of the feasible solution. The approach outlined in the following chapters will be sufficiently-generic so as to allow for this approach to be applied to other situations.

CHAPTER 2 SOLUTION DEVELOPMENT

2.1 Approach Overview

Before diving into the details of the design, a quick summary follows. Each topic introduced in the next few paragraphs is discussed more-fully in the following sections.

The design process for the K15 beam flattener centered around a numerical analysis of the radiation beam. Radiation exits the linear accelerator in a continuous pyramid of radiation, which is very difficult to computationally analyze in its true form. For the purposes of this project the beam was considered instead to consist of a finite number of individual rays. While this was an accurate representation of the paths followed by radiation photons, it was not a truly correct model of the beam itself. This simplification does, however, enable a much simpler method of analysis and was considered to be more than adequate for this project's needs.

Following the beam discretization, absorption was calculated along each ray. Theoretically, an even exposure would result from each ray traversing the same amount of material. By comparing the material experienced by each ray it is then possible to determine how much extra material must be added to that ray to cause it to be equal to each of the others.

This approach provided the basis for the design and was considered to meet the desired accuracy. Due to the complex modeling required to account for the scattering effects described in sec. 1.1.2, the issues of scatter and neutron radiation were not addressed in this design. Most of the radiation experienced by the detector is from the linear accelerator itself, allowing the analysis focus to remain on the radiation emitted from the source rather than becoming concerned with scatter. Additionally, unrelated experimental data has shown that neutron radiation is not an issue at the detector plane, which allows not considering the effects of the neutrons.

2.2 Assumptions

A few key assumptions were made in the modeling of this problem and are listed here for easy reference and will be discussed more fully in the following sections.

1. Photons were assumed to travel in a straight line, regardless of the material through which it was passing. It was also assumed that there would be no change in direction at material interfaces (i.e., no refraction).
2. All radiation was assumed to have been emitted from a point source.
3. It was assumed that an accurate model of the beam could be generated through the use of a sufficiently-large number of discrete rays.

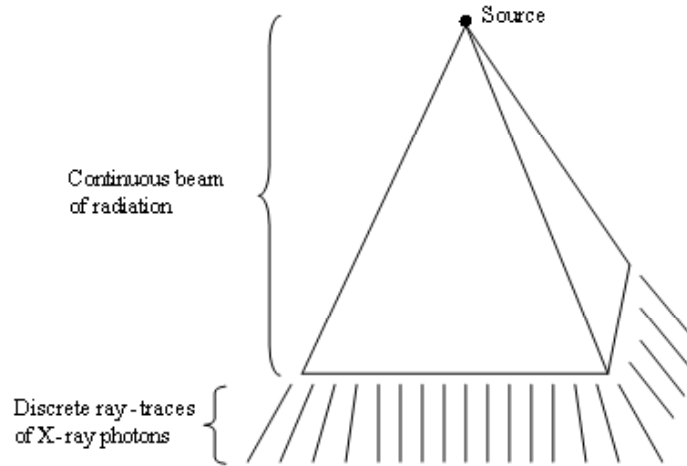


Figure 2.1 Discretizing the continuous cone of radiation

2.3 Beam Modeling

2.3.1 Continuum to Discrete

Generating the mathematical model for the radiation beam itself required two key components. First, the beam could not be analyzed as the continuous cone of radiation as it actually exists. Instead, this continuum of radiation had to be modeled as a fine set of discrete rays. This resulted in a model based upon numerical-analysis rather than a closed-form analytic solution. While a closed-form solution would provide greater accuracy, the difficulty associated with such an effort would have required more time than the project was allotted. The loss in accuracy due to the numerical approach was countered by the use of large numbers of rays (on the order of 10^4) in the analysis. As the number of rays analyzed increases the model will become closer and closer to the true physical situation. Thus, by choosing a sufficiently-large number of rays for the analysis it was possible to incorporate the necessary accuracy into the model.

During the design process several resolutions of discrete rays were compared before choosing 10^4 as the optimum order of magnitude. At lower orders of magnitude the calculated models still had the same basic shape, but a less smooth surface. The surface became smoother with the inclusion of more rays and the best balance of calculational precision and model practicality was determined to occur with ray counts on the order of 10^4 . This was enough rays to have high accuracy in the model without exceeding the computer's resources.

Two assumptions were associated with this radiation model. First, the rays were assumed to be straight, with no refraction at the interfaces between materials. This assumption was made using experimental data and observations made during the course of two decades of inspections. And second, all rays were assumed to originate from a point source. While the source size is finite and known, modeling effort is greatly reduced if the source is instead considered to be a singular point. True source size is used in various inspection calculations (such as unsharpness), but the effects of the source size were considered to be negligible in this application due to its very small size with respect to the other setup parameters.

Each ray was defined as originating from the singular source and propagating to the detector plane at two specified orientation angles. These angles are discussed further in sec. 2.4.1. Generating

the set of rays for the analysis was accomplished by simply defining the angle range across which to sweep and the angular increment between each ray.

2.3.2 Intensity Variation

The other key component affecting the beam modeling was the varying radiation intensity as a function of spatial location. This concept was introduced in 1.1.1. In the case of rocket motor inspections, the intensity profile exiting the linear accelerator is not compatible with the geometry of the components being inspected. It is this incompatibility that necessitates the use of a beam flattener and also the reason why the beam intensity must be included in the mathematical model.

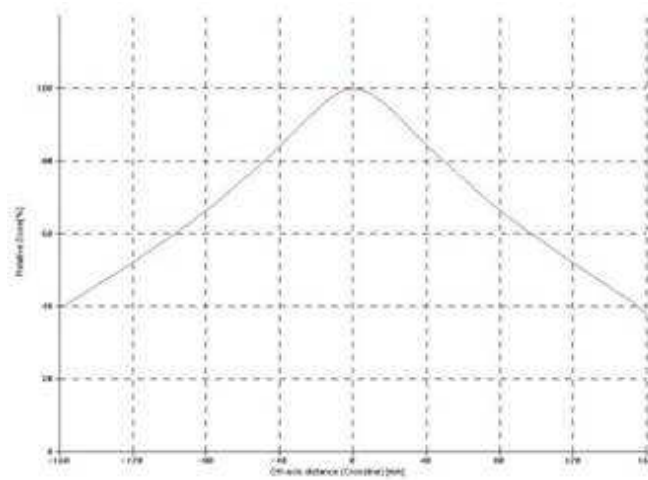


Figure 2.2 Beam intensity profile

The beam intensity profile was previously known due to measurements conducted as part of the installation and validation procedure. A plot of the intensity profile as a function of horizontal position at the front of the accelerator can be found in fig. 2.2. It was determined that the intensity profile could be accurately-approximated as being linear and symmetrical with respect to the beam centerline. This linear approximation allowed for simple calculations to determine the intensity of each ray. Incorporating this profile into the beam model was accomplished through the use of HVLs (introduced in sec. 1.1.1). The model simply added the appropriate number of HVLs to produce the intensity which had been measured at that point. For example, if a particular ray was known to have an intensity of one-half the centerline value, one HVL was added to this ray. Since the HVLs experienced by each ray are summed, it is irrelevant as to where each HVL is encountered. The key issue is for each ray to experience identical numbers of HVLs and therefore equal absorption.

2.4 Hardware Modeling

2.4.1 Coordinate System

Accurate calculations depend upon a consistent coordinate system. In order to avoid errors resulting from constant transformations between coordinate systems, a global system was defined. The origin was chosen to be at the radiation source. The location of the origin is an arbitrary choice and therefore any position will work so long as everything remains consistent with that choice.

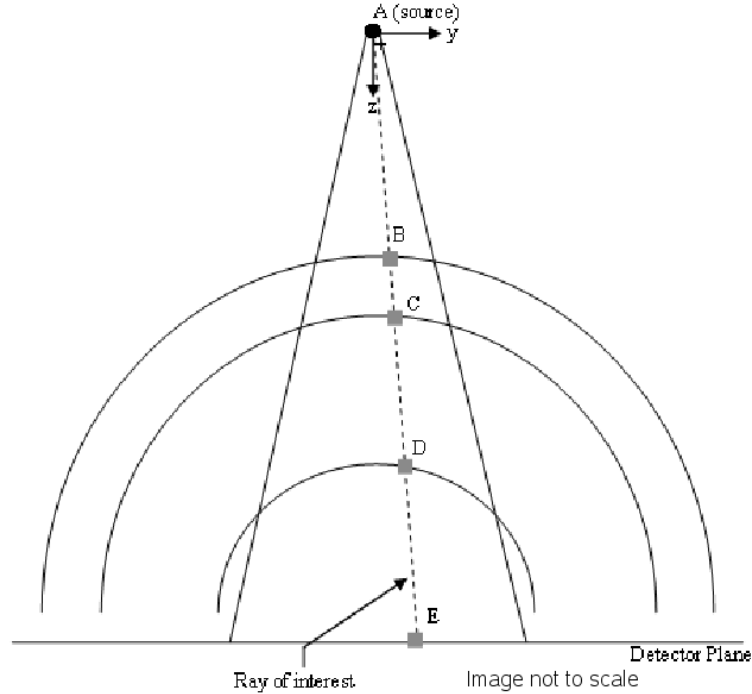


Figure 2.3 Points of interest in modeling the hardware

Choosing the source as the origin made defining the ray angles introduced in sec. 2.3.1 straightforward. All angles were defined as positive using the right-hand rule, consistent with engineering convention. In the case of the rays, they were defined by two angles, one being the angular distance from the beam centerline along the longitudinal axis of the rocket motor and the other being the angular distance from the beam centerline as measured perpendicular to the longitudinal axis. The use of these two angles to define the ray orientation is analogous to working in a spherical coordinate system.

All coordinates used in calculations were in this global system. Fig. 2.3 depicts a ray passing through several layers of material within a component. The points A through E in this figure were all found in terms of the global coordinate system, which allowed for straightforward calculations as detailed in sec. 2.4.2.

2.4.2 Defining The Geometric Model

In addition to accurate beam modeling, accurate modeling of the inspected components is also essential. This mathematical model is based on calculating the number of HVLs experienced by each ray, which is understandably heavily dependent upon component geometry. As mentioned in sec. 1.1.1, HVLs are not solely dependent upon material thickness. The radiation absorption characteristics of each material must also be known in addition to the material thicknesses.

Before material thicknesses could be determined, the material locations had to first be defined. Using the coordinate system discussed in sec. 2.4.1, the location of each material interface was calculated as a function of ray orientation. This proved to be the most difficult aspect of the project due to the interaction between the straight rays and the curved rocket motor geometry. Through careful equation development, aided by the MATLAB Symbolic Math Toolbox, the necessary equations were developed but cannot be discussed here due to restrictions discussed in

appendix B. For the purposes of this report, discussion will continue with the understanding that the coordinates of each intersection between material and ray are known.

The following generalized equations provide the basis for the mathematical model of the inspected components.

$$ds = \sqrt{(x_2 - x_1)^2 + (y_2 - y_1)^2 + (z_2 - z_1)^2} \quad (2.1)$$

$$\lambda = \frac{ds}{\mu} \quad (2.2)$$

$$\Lambda = \sum_{i=1}^n \lambda_i \quad (2.3)$$

In equation 2.1 ds is the distance the ray travels through a particular material. In this case the material thickness is defined by the coordinates at which the beam enters the material, (x_1, y_1, z_1) , and exits the material, (x_2, y_2, z_2) . This equation is simply the geometric distance equation, also known as Pythagorean's Theorem, in three dimensions.

Equation 2.2 demonstrates how the HVL was calculated for a particular ray through a given material. Here, ds is the same as in eqn. 2.1 while μ is the thickness of one HVL for the given material. This equation outputs λ , which is the number of HVLs experienced by the ray through this material.

For each ray, the HVLs experienced while passing through each material are then summed as in eqn. 2.3. In this equation n is the number of individual materials through which the ray must pass while Λ is the total number of HVLs experienced by the ray.

2.5 Flattener Determination

Once both the beam and components had been modeled it was possible to calculate the necessary flattener geometry. This was an inverse process as compared to the HVL calculations performed above, but the same governing theory applies. The flattener must provide enough material for each ray to account for the differences in HVLs experienced due to the component geometry, so now instead of solving for the number of HVLs the ray encounters the calculations are now to determine the distance the ray must pass through the flattener in order to equate it to all other rays.

2.5.1 Surface Calculations

The front face of the beam flattener was defined to be a flat plane perpendicular to the beam centerline. This was necessary for mounting the flattener within the K15. With this face defined, all that remained was to define the back side according to the requirements of each ray. As introduced above, this was determined using the opposite process from sec. 2.4.2. In these calculations the HVL requirement was known and defined to be the number of HVLs that would make this ray equal to the most-absorbed ray in the beam. Knowing this, the following equations were applied.

$$\lambda_{req.} = \Lambda_{max} - \Lambda_i \quad (2.4)$$

$$ds_{flattener} = \lambda_{req.} \mu_{flattener} \quad (2.5)$$

Again, $\mu_{flattener}$ is the thickness of the HVL for the flattener material (discussed in sec. 2.5.2), while Λ_i is the number of HVLs experienced by the ray before the flattener is included, and

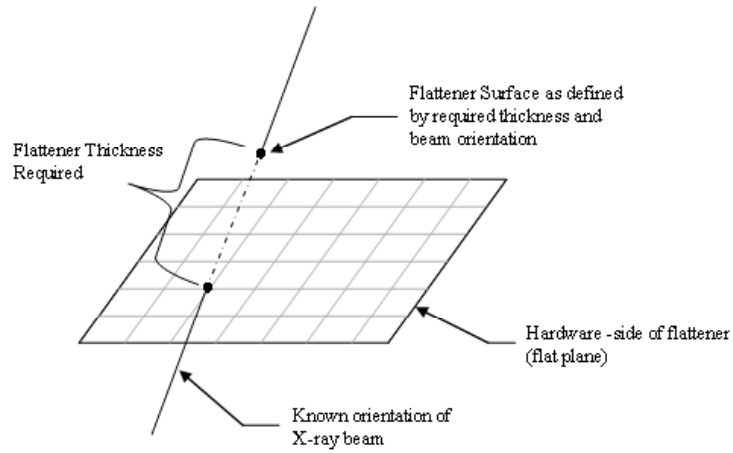


Figure 2.4 Determining the flattener top surface

Λ_{max} is the number of HVLs experienced by the most absorbed ray. The flattener thickness is a function of, but not equal to, $ds_{flattener}$, which is the distance the ray must travel through the flattener. This distance is not equal to the thickness due to the orientation of the ray. By knowing the orientation angles of the ray and the required distance through the flattener it is possible to define the back surface as represented in fig. 2.4.

2.5.2 Material Selection

Tungsten was chosen as the material to use for the beam flattener. The large density of tungsten gives it tremendous radiation stopping power, which was desirable considering the limited space within the K15. The biggest drawback related to tungsten comes from its tendency to emit neutron radiation at high radiation energies. However, experimental data revealed that neutron radiation was not striking the detector plane. This led to the conclusion that tungsten could be used as the flattener material despite its neutron radiating tendencies.

2.5.3 Fabrication Data

Using the procedure outlined in this chapter, the flattener surface was fully-defined. Fabrication, though, requires coordinate data. The coordinates that define the back surface were written into a data file that could then be passed along to the manufacturing facility which would produce the flattener.

CHAPTER 3 FINAL DESIGN

3.1 Idealized Design

Using the procedure outlined in the previous chapter a fine-mesh model of the beam flattener was developed and can be seen in fig. 3.1. The term “fine-mesh” is used due to the large number of rays used in the analysis. The density of the rays was on the order of one hundred rays per degree. Qualitatively this model appeared to have merit based on key features:

1. The curved surfaces about the long axis appear reasonable considering the curved hardware for which the beam flattener is designed.
2. The linear slopes from the center to the short edges are expected due to the constant hardware dimensions in this direction and the increasing effective material thickness due to the ray angles.
3. The ridges from the center to the corners are expected as a result of the beam intensity modeling. The pyramid-like beam intensity model causes the flattener to compensate that profile.

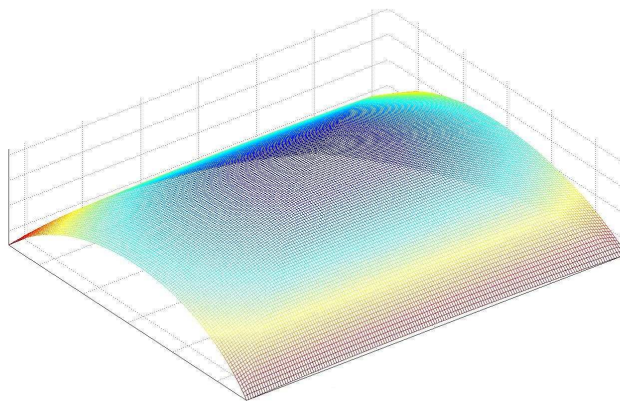


Figure 3.1 Isometric view of fine-mesh model

Although this model looked fantastic and had many qualities which implied accuracy, it was not feasible to produce. The surface was too complex with its continuously-changing curvatures. Over 20,000 points were used to generate this model and fabrication would have required multiple weeks of effort on highly-sophisticated milling machines. This intense effort is due to the difficulties associated with machining tungsten. Neither the timeline nor the project budget could justify such an effort.

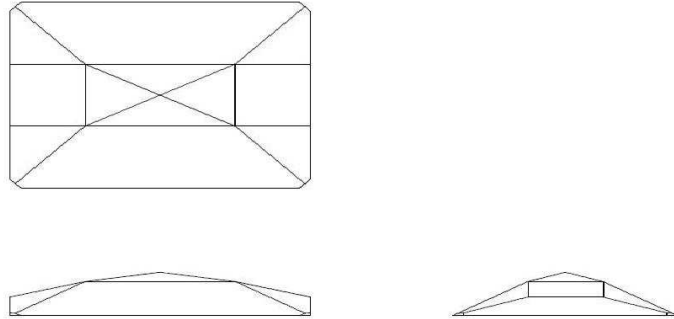


Figure 3.2 Orthogonal views of the simplified flattener design

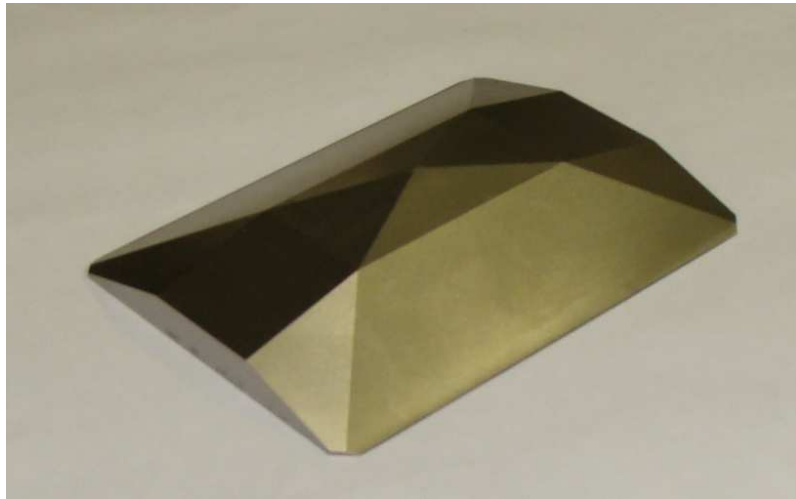


Figure 3.3 Photo of new beam flattener

3.2 Design Simplification

Simplifying the design transformed this project from including only numerical analysis to encompassing an element of intuition. In order to generate a manufacturable design the contoured surface had to be simplified by several orders of magnitude. The original twenty-thousand-plus points defining the complex curves and ridges of the surface had to be reduced to less than fifteen. The results of this simplification can be seen in fig. 3.2 and a photograph of the actual installed flattener can be seen in fig. 3.3.

This massive vertex reduction was accomplished by combining both the ideal design and the original flattener's design. The original flattener design was used as a basis for the simplified form of the new flattener. Naturally, the vertex coordinates would be different, but qualitatively there would be many similarities between the two flatteners. Once the key points were identified using the old flattener, dimensions from the new design could be taken and used to define the new, simplified flattener.

3.3 Design Performance

Flattener performance was determined by comparing film exposures for identical inspections on identical components taken before and after flattener installation. Comparison data were collected for three hardware configurations: old linear accelerator with the old flattener, new linear accelerator with the old flattener, and new linear accelerator with the new flattener. Film exposures were measured at 81 points per exposure and were compared using both statistical and graphical methods. The data collection points are visualized in fig 3.4.

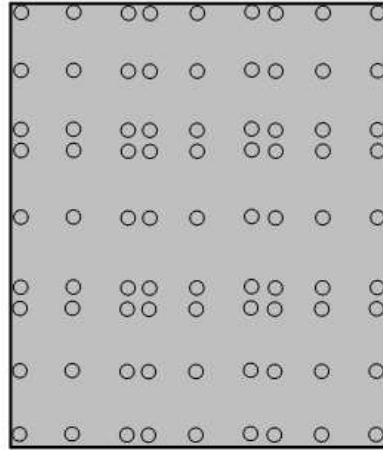


Figure 3.4 Exposure data collection locations

In addition to the statistical analysis described in sec. 3.3.1, a qualitative graphical comparison was performed by generating plots depicting the varying film exposures, found in sec. 3.3.2. Instructions for interpreting these plots can be found in appendix A.

3.3.1 Statistical Analysis

Numerical exposure data were compared between identical geometric setups with varying inspection hardware. The results can be found in table 3.1. As seen in the table, the new linear accelerator demonstrated a significant decrease in performance when used with the old beam flattener. Significant rises in both exposure range across the film array and the standard deviation of the data set indicate that although exposure levels still fell within the allowable ranges, the quality of the inspection was not equal to the historical standard.

Following the installation of the redesigned flattener the same test shots were taken and compared. When comparing the K15 with the new flattener to the historical standard it was found that both exposure range and standard deviation decreased. While these decreases were not as dramatic as the increases witnessed with the old flattener, they do indicate an improved inspection process. When searching for defects a technician will better-perform with film that has a more-even exposure, such as the K15/new flattener combination.

3.3.2 Graphical Analysis

Graphically, the exposures described above can be represented by generating three-dimensional plots as described in appendix A. The first plot to examine is that of the L6000 with the old flattener. This combination had been in use for over twenty years before the K15 installation project and it sets the baseline for inspection quality standards.

| Linear Accelerator | L6000 | K15 | Percent Change | K15 | Percent Change |
|--------------------|---------------------|---------------|-----------------|--------------|-----------------|
| Beam Flattener | Old | Old | (From Original) | New | (From Original) |
| Exposure Range | 1.02 | 1.42 | +39.2% | 0.91 | -10.8% |
| Standard Deviation | 0.26 | 0.37 | +42.3% | 0.20 | -23.1% |
| | Historical Standard | First Attempt | | Final Design | |

Table 3.1 Statistical comparison

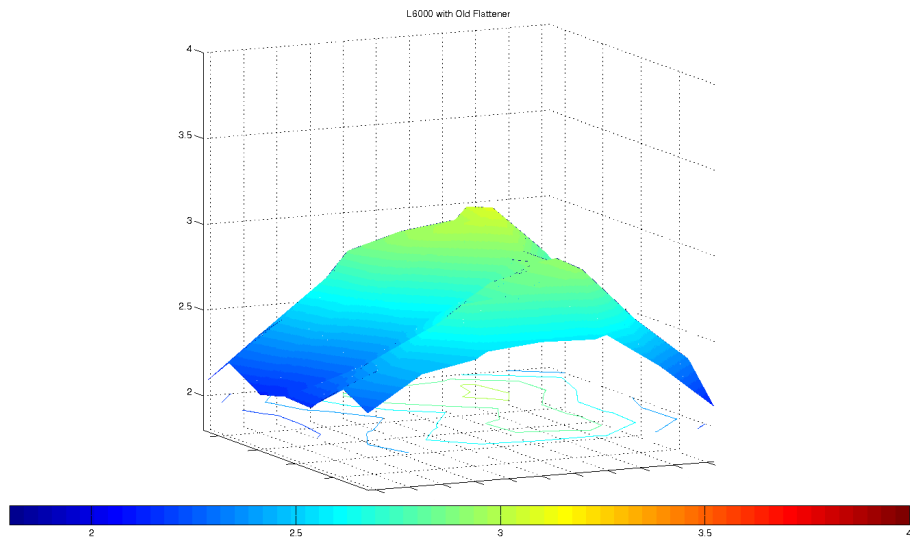


Figure 3.5 L6000 with old beam flattener surface plot

As seen in fig. 3.5, there is a double-peak in intensities near the center due to the old flattener's peak not accurately compensating for the intensity peak of the L6000.

Fig. 3.6 shows the increased exposure range along with the same double-peak observed in the L6000 case. The steeper slopes on this plot translate into a more distinct gradient from dark to light on the x-ray film and a more-difficult job for the interpreting technician.

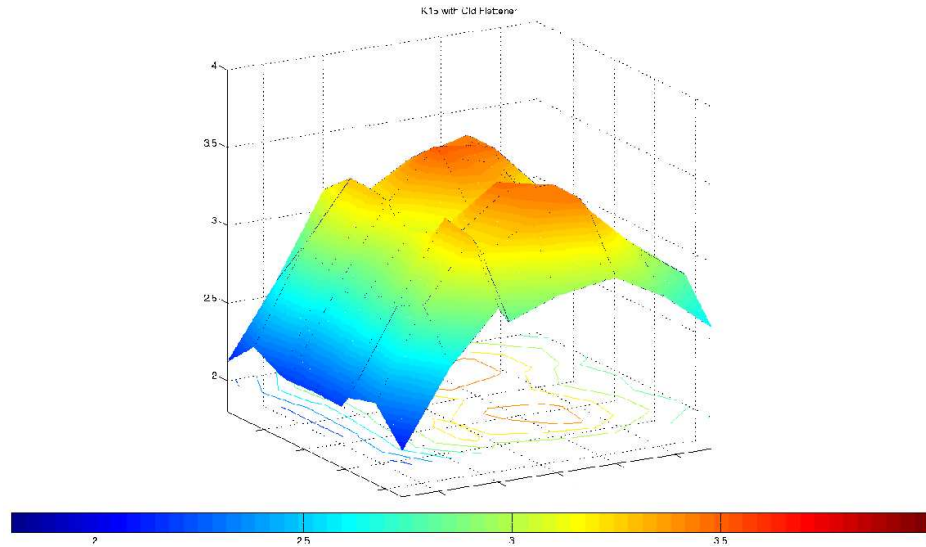


Figure 3.6 K15 with old beam flattener surface plot

In fig. 3.7 the improvements made using the new beam flattener can be observed. While the contours of the plot are not as consistent as those using the old flattener, the overall effect is one of a more-even exposure. Flattening the beam in the center has been greatly-improved, although the double-peak still exists and now appears on the edges of the film array. The wide, flat portion in the middle of the array will provide technicians with an improved background from which to search for defects and the rises along the edges are not so large as to cause difficulties.

Using similar plots as found in figs. 3.5, 3.6, and 3.7, this time viewed orthogonal to the film array, it becomes easier to see both the reduced performance of the K15 with the old beam flattener and the performance gained through the new beam flattener. This comparison is found in fig. 3.8. The K15 plot in the middle shows the greater range in colors and faster change between colors, indicative of a poorly-flattened beam. The L6000 plot on the left, while not perfect, is distinctly better than that of the center image. The plot on the right was generated by the K15 and the new beam flattener. From this plot one can see the more-even color range, indicating a smaller exposure range and improved inspection performance.

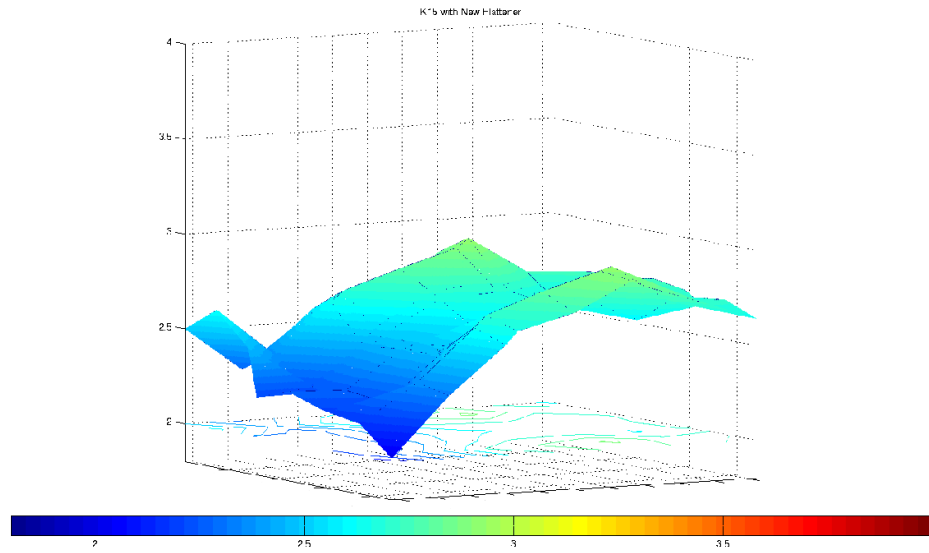


Figure 3.7 K15 with new beam flattener surface plot

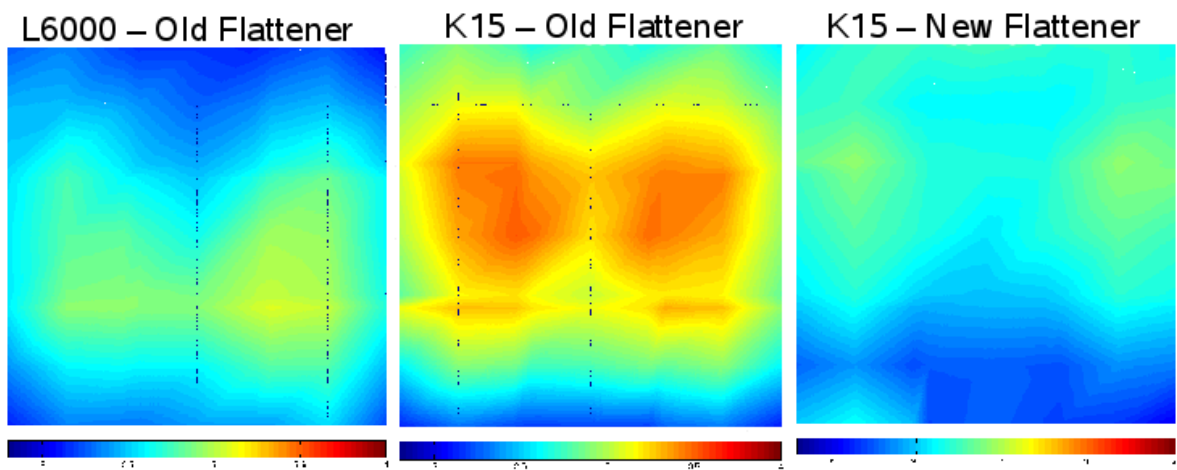


Figure 3.8 Exposure Comparison Plots

CHAPTER 4 CONCLUSIONS

4.1 Quantitative

As presented in sec. 3.3.1, the new beam flattener did produce a statistically-improved inspection. Both exposure range and standard deviation were reduced from the historical standard and proved to be a substantial improvement over the old flattener installed in the new linear accelerator.

4.2 Qualitative

From the graphs presented in sec. 3.3.2 it was again seen that the new beam flattener provided observable gains in performance over the existing hardware. While a perfect, flat plane was not produced in the exposure maps, the terrain was visibly smoothed-out and less steep.

Additionally, feedback from the technicians performing the inspections has been overwhelmingly positive.

4.3 Final Verdict

Combining this operational perspective with the numerical and graphical data already discussed leads to the conclusion that this beam flattener redesign project has been a success. Additionally, the data validates the analytical approach outlined in this report and suggests that it could be applied to other applications and scenarios.

4.4 Future Work

Since the film exposure plots for the new flattener do not depict a flat plane, there is still work to be done in regards to improving the analytical methods for high-energy radiation. This model did not consider scatter effects, and no calculations were done to anticipate film exposures using the simplified flattener. Most future work related to this project would need to take one of two paths:

1. Model the new, simplified flattener and calculate the theoretical film exposure. This would be a valuable test in analyzing the validity of the numerical analysis method as it would allow a direct comparison between computer calculations and experimental results.
2. Develop a model for scatter radiation. Given the complex, non-linear nature of the calculations required for this, modeling scatter would be quite a feat. However, accurate simulation of scatter radiation would serve to further-enhance the ability to predict and model inspection scenarios. With a scatter simulation included in this project the flattener may well have performed even better due to the improved model of the physics involved.

This design has proven successful enough to warrant the application of a similar approach to both new components and different inspection geometries. Work has already begun at ATK Space Systems to apply the design process discussed in this report to these new inspections.

4.5 Significance

The importance of this project's success goes farther than simply showing a decrease in film exposure ranges. The meaning of these results must be understood, as well as how they translate to the rocket motor's end users: United States Astronauts.

The combination of the old beam flattener and new linear accelerator required extra exposures for each portion of the inspection process in order to meet film exposure requirements. These additional exposures required by the old flattener caused budget, resource, scheduling, and delivery problems, as well as frustrations on the part of the technicians who used it. However, after installing the new beam flattener no extra exposures were required, solving the logistical and financial problems imposed by the old design.

4.5.1 Inspection Quality

By improving the medium by which technicians determine motor quality this new flattener serves to enhance the inspection as a whole. Smaller variations in background exposure will result in an increased detection ability and allow for a more-accurate understanding of each motor's unique characteristics. Additionally, better image quality will reduce the need for reshooting exposures. This will reduce both film and development chemical costs, in addition to saving valuable time.

4.5.2 Safety

All the improvements translate into one overarching goal: safety. As a producer of the largest human-rated solid-fuel rocket motors in the world, safety is the number-one priority of ATK Space Systems. The improved inspection process, as facilitated by this new beam flattener will help increase the safety of the solid rocket boosters that pass through the inspection bay.

APPENDIX A INTERPERETING FILM EXPOSURE PLOTS

Graphically analyzing the film exposure levels between each combination of linear accelerator and beam flattener required the development of a new analysis tool. The use of MATLAB, and its powerful graphics capabilities, allowed for the quick-generation of plots depicting the film exposure as a function of location on the film array.

The horizontal and vertical axes are arbitrary and were chosen to be the coordinates on the film board array. These dimensions are not shown within this report as they are not important to the interperetation of the plots.

Surface plots are shown from two perspectives: tri-metric and orthogonal to the film array. In the tri-metric view the vertical axis on each surface plot is the film exposure as measured in H & D units, a standard measure of film exposure. The surface is also color-coded to assist in assessing the various levels of exposure.

The orthogonal plots only show the colors, which change proportional to the exposure levels. The fade from red (large values) to blue (small values) is representative of the film changing from less-transparent (high exposure) to more-transparent (low exposure). All colored plots have been scaled such that the colors range from exposure measurements of 1.8 to 4.0 H & D units.

One must keep in mind that in an ideal situation the film exposure would be even across the entire film array. Due to the effects of scatter and non-zero tolerances in the exposure setup a variation in exposures is expected and observed in each image.

APPENDIX B INTERNATIONAL TRAFFIC IN ARMS INFORMATION

Much of the data related to this project fall subject to International Traffic in Arms (ITAR) regulations. Any and all data that is considered restricted by these regulations has been removed from this document. Most-often this is noticed in the form of images having no dimensions. In addition to dimensions being removed, technical drawings of the beam flattener and computer-generated models have been modified and are no longer to scale.

While the removal of these details may result in less-smooth wording at various points within this report, it is necessary and in the interests of national security. The purpose of this paper was to explain the process used in the design of a high-energy beam flattener, which is independent from the details of its implementation.

In addition to dimensionless images, very few equations are to be found in this report. Most equations are dependent upon the unique situation in which they are applied, such as modeling the component geometries, and are therefore subject to ITAR restrictions. Along with the imposed restrictions, such equations would be of no use to the general reader as they would not assist in the modeling of the reader's application of interest. As such, development of nearly all modeling equations are left to the reader.